Downloaded 09/09/15 to 62.252.55.50. Redistribution subject to SEG license or copyright; see Terms of Use at http://library.seg.org/

Dynamic angle and azimuth decomposition of RTM images

N. D. Whitmore, Sean Crawley, Chaoguang Zhu, Armando Sosa, PGS*

Summary

In the application of reverse time migration (RTM) to wide and full azimuth data, it important not only to produce a final RTM image, but also to decompose the data into pre-stack gathers that can be used both for processing and tomography. We discuss here a method where the RTM image can be mapped into angle-azimuth gathers by direct binning at each time step, where the RTM backscattered noise is minimized during the propagation process by the application of an inverse scattering imaging condition. We demonstrate the angle-azimuth decomposition to the application of RTM imaging and 3D angle tomographic model building in wide azimuth data from the Gulf of Mexico. Also, in preparation for the processing of a full azimuth survey in the Gulf of Mexico, we also examine the angle-azimuth decomposition for 3D RTM imaging using a full azimuth 3D synthetic based on the SEG SEAM model.

Introduction

Reverse time migration (RTM) has become a standard method for illumination of complex geologic structures and potential reservoirs. To more fully make use of the angular and azimuthal coverage of the wide azimuth acquisition systems, imaging and velocity estimation methods require adequate treatment of subsurface dip, azimuth, and illumination angle. However, in order to provide data for the data processing and 3D tomography, it is necessary to decompose the prestack image into gathers that sample both the azimuth and angular components of the image. In this paper we focus on an RTM imaging method that decomposes the prestack image into surface angle and azimuth gathers, which allows for subsequent angle and azimuth based processing and the application 3D wide azimuth tomography for model building .

There are number of approaches to the generation of RTM angle gathers (e.g. Zu, Zhang, and Tang, 2011). We present here an RTM image decomposition method, which is a dynamic binning onto angle and azimuth, done at each time step. The method employs inverse scattering imaging conditions to reduce backscattered noise during propagation (Whitmore and Crawley, 2012), which is essential in providing high quality angle gathers.

RTM Angle – Azimuth Gather Decomposition

Reverse time migration (RTM) is a shot based migration method, where each shot is imaged onto the subsurface independently. During the imaging process, the source and receiver angles can be determined from a combination of the source wavefield direction vectors and subsurface dip (or alternatively, the receiver wavefield direction vectors at the source onset time), giving an opening angle computation given by equation (1), where Ps and Pr are the direction vectors computed directly from the wavefields and subsurface dip.

$$\theta(\mathbf{p}_S, \mathbf{p}_r) \cong \frac{1}{2}\cos^{-1}\left(\frac{\mathbf{p}_S \bullet \mathbf{p}_R}{|\mathbf{p}_S||\mathbf{p}_R|}\right) \quad (1)$$

However, angular decomposition of the RTM image requires removal of the backscattered RTM noise at each time step, which cannot be done by standard correlation based imaging conditions (where the backscattered noise interferes with the decomposition of the data). To mitigate this problem, we employ an advanced imaging condition, which we refer to as an inverse scattering imaging condition (ISIC). The ISIC imaging condition at a fixed time t is shown in equation 2(a) (Whitmore and Crawley, 2012; Stolk, et al, 2009), where (2b) are the source and receiver wavefields in the frequency domain.

$$\hat{I}(\mathbf{x},t) = W_1(\mathbf{x},t)\nabla\Psi_S(\mathbf{x},t) \bullet \nabla\Psi_R(\mathbf{x},T-t) + W_2(\mathbf{x},t)\frac{1}{v^2(\mathbf{x})}\frac{\partial\Psi_S(\mathbf{x},t)}{\partial t}\frac{\partial\Psi_R(\mathbf{x},T-t)}{\partial t} \quad (2a)$$

$$\hat{\Psi}_S(x,\omega) = \omega^{-(\alpha+1)/2}\hat{P}_S(\mathbf{x},\omega)$$
$$\hat{\Psi}_R(x,\omega) = \omega^{-(\alpha+1)/2}\hat{P}_R(\mathbf{x},\omega) \quad (2b)$$

This imaging condition uses two imaging kernels, which when combined largely attenuate the backscattered RTM noise. This generates a backscatter free RTM image that can be decomposed into subsurface angles via the decomposition described in equation 2. At the same time, the RTM image can also be binned onto output azimuth bins - allowing for a direct mapping to angle-azimuth images during RTM imaging as shown in equation 3.

$$\hat{\hat{I}}(\mathbf{x}_S, \mathbf{x}, \theta, \alpha, t) = Bin_{\theta,\alpha}(\hat{I}(\mathbf{x}_S, \mathbf{x}, t)) \quad (3)$$

Where θ = angle, α = azimuth, **x**=(x,y,z)

The final RTM angle-azimuth images are then computed by summing the binned images over all time and then over all of the resultant shot images as shown in equation 4.

$$I(\mathbf{x},\theta,\alpha) = \sum_{x_S}\int A(\mathbf{x},\theta,\alpha)\hat{\hat{I}}(\mathbf{x}_S,\mathbf{x},\theta,\alpha,t)dt \quad (4)$$

This dynamic angle-azimuth decomposition of the RTM image is achieved during the RTM computation and angle-azimuth data is saved at each image point. This allows for post migration processing such as residual depth error corrections, angle and azimuth dependent stacking, and 3D tomography. Note that the angular sampling at a specific

© 2014 SEG

DOI http://dx.doi.org/10.1190/segam2014-0876.1

Downloaded 09/09/15 to 62.252.55.50. Redistribution subject to SEG license or copyright; see Terms of Use at http://library.seg.org/

image point depends directly on the spatial sampling of the acquisition system. If regularly sampled angle gathers are required for analysis, as in the case of 3D tomography, some form of specular resampling may be required (e.g. Tang, et al., 2011). In the examples shown here, no resampling has been done,

Example: 3D wide azimuth RTM - GOM

3D TTI anisotropic RTM was applied to a 3D Gulf of Mexico wide azimuth (WAZ) survey. This survey has an inline offset of 8 km, a crossline offset of 2 km and a sail line spacing of 600 meters. The data was decomposed into 4 azimuths with 2 degree angle images for each azimuth.

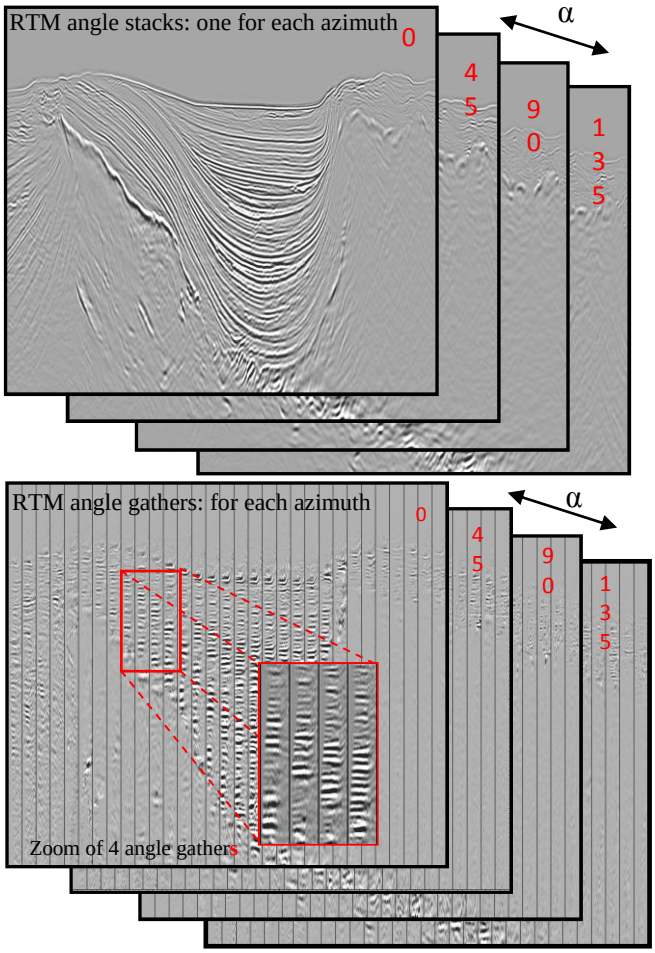

Figure 1: TTI anisotropic RTM depth migration angle stacks and angle gathers (0-40 degrees) for azimuths 0, 45, 90, 135 degrees from a wide azimuth survey recorded in the Gulf of Mexico. These are computed by the imaging process of RTM propagation, inverse scattering imaging condition and angle-azimuth binning and stack. The zoom is of 4 gathers at different spatial locations, with 0-40 degrees within each gather.

Examples of the stacked RTM image and angle-azimuth decompositions are shown in Figures 1 and 2. Figure 1 shows examples of both the angle stacks and angle gathers for each azimuth. Figure 2 shows the full RTM depth migration stack, which is computed by summing over all angles and azimuths. Also shown in Figure 2 is a set of full angle-azimuth gathers, where the full range of angles and azimuths are shown at each (x,y) location The angle gathers shown are for angles of 0-40 degrees, and azimuths of 0, 45, 90, and 135 degrees.

While only selected images are shown here, the full set of angle-azimuth data is computed and saved for all (x,y,z) in the output image space, allowing for optimized stacking and angle and azimuth dependent attributes.

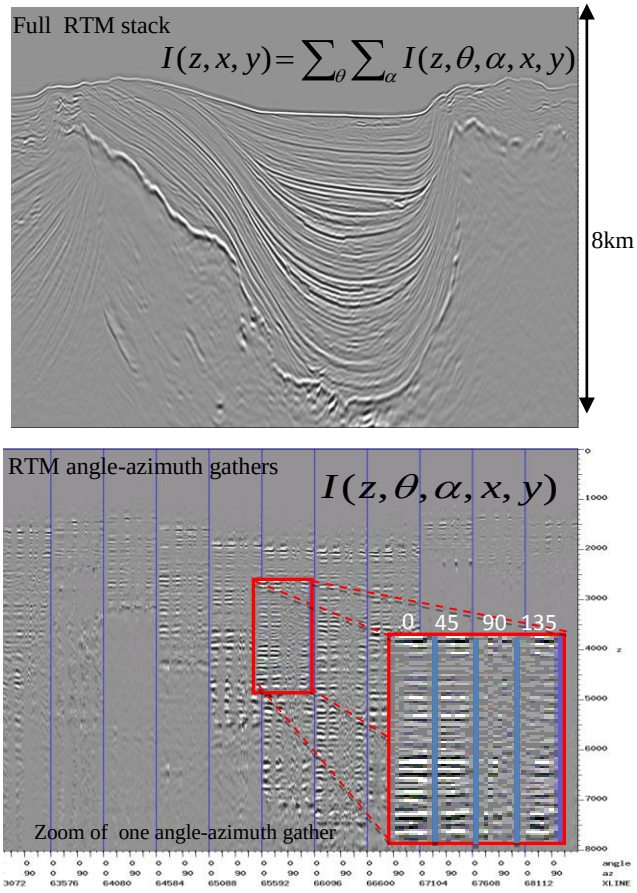

Figure 2: Full RTM TTI anisotropic depth migration stack and RTM angle-azimuth gathers. The stack was performed by summing all of the data within each angle-azimuth gather. Each angle-azimuth gather has data for angles 0-40 degrees and azimuths 0, 45, 90, 135 degrees. Note the 90 degree azimuth is poorly sampled, due to the 600 meter sail line spacing.

© 2014 SEG

DOI http://dx.doi.org/10.1190/segam2014-0876.1

Downloaded 09/09/15 to 62.252.55.50. Redistribution subject to SEG license or copyright; see Terms of Use at http://library.seg.org/

Example: 3D RTM angle tomography – WAZ GOM

In addition to the generation of optimized stacking from the angle-azimuth decomposition of the 3D RTM images, residual depth errors can be computed and projected onto model based updates using angle based tomography.

The equation setup for the angle-azimuth tomography systems employ upward ray tracing, using the subsurface angles and azimuths determined by the RTM angular decomposition and subsurface dip (see Figure 3).

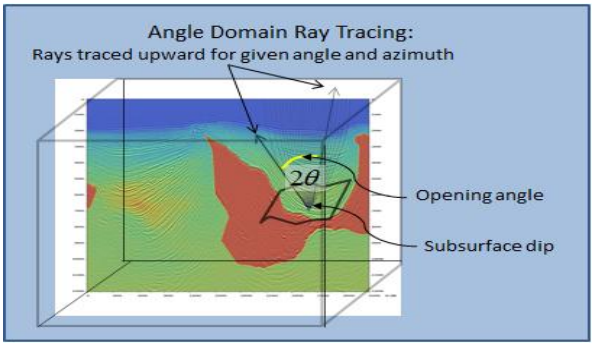

Figure 3: RTM angle domain tomography uses travel times computed by ray tracing upward from reflection points in the subsurface for a set of angles, azimuth and subsurface dip.

The tomographic process includes several steps – gather conditioning, residual depth error estimation, ray tracing, tomographic equation setup, and tomographic inversion as show below:

1. Compute travel times within a single cell:

$$t = \vec{p} \bullet \vec{l} = sl\cos\phi$$

2. Linearize to compute Δt as a function of parameters:

$$\Delta t = \left(\frac{\partial s}{\partial s_{p0}} \Delta s_{p0} + \frac{\partial s}{\partial \varepsilon} \Delta\varepsilon + \frac{\partial s}{\partial \delta} \Delta\delta \right) l\cos\phi$$

3. Use a conjugate gradient method with regularization to solve the tomographic system that minimizes

$$\varphi = \|\mathbf{b} - \mathbf{A}\mathbf{x}\|^2 + \tau_s \|\mathbf{R}_s \mathbf{x}_s\|^2 + \tau_\varepsilon \|\mathbf{R}_\varepsilon \mathbf{x}_\varepsilon\|^2 + \tau_\delta \|\mathbf{R}_\delta \mathbf{x}_\delta\|^2$$

The 3D angle based tomography was applied to the 3D wide azimuth survey discussed above. The RTM imaging and angle-azimuth imaging was applied using a starting model, residual depth errors were computed, and 3D tomographic inversion was applied. This process was applied to two full RTM imaging and tomography iterations.

A small subset a single azimuth gathers and the starting and final tomographic model were extracted for display and are shown in Figure 3 below. The gathers are displayed with their respective velocity models. While the migration was a full TTI model, only the velocity field was updated in this example.

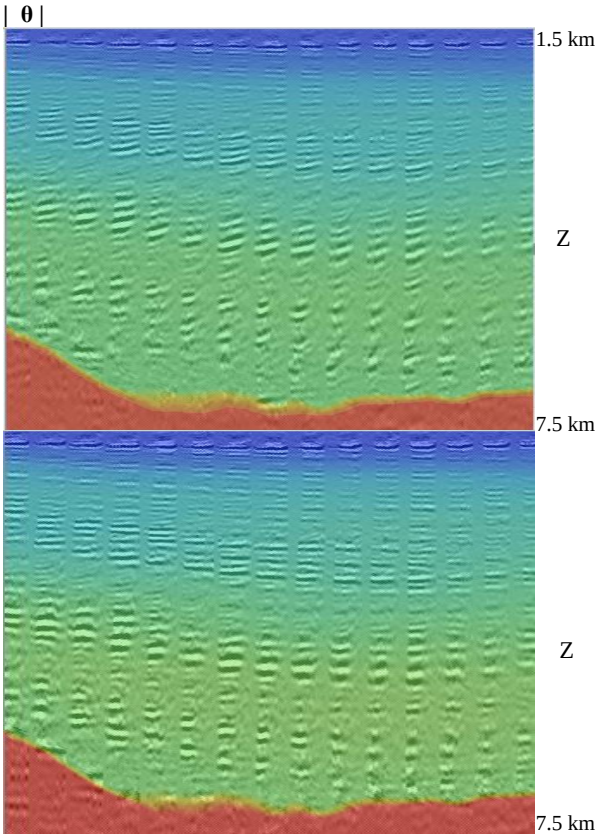

Figure 4. Two iterations of 3D RTM imaging with angle-azimuth decomposition and angle based tomography was applied to the 3D GOM wide azimuth survey discussed above. For each iteration the depth residuals were picked and a tomographic update was performed. Starting and final (single azimuth) gathers are shown above.

Example: Full azimuth RTM – 3 azimuth SEAM Model

To prepare for full acquisition in the Gulf of Mexico, a detailed model study was created using the SEG SEAM model. Three wide azimuth finite difference synthetics were generated and imaged with 3D RTM. Each azimuth was imaged independently and dynamically binned into 3 image azimuths, which created imaged data with angle images for each of the 3 image azimuths (0, 60 120 degrees) x 3 acquisition azimuths (0, 60, 120 degrees).

© 2014 SEG

DOI http://dx.doi.org/10.1190/segam2014-0876.1

Downloaded 09/09/15 to 62.252.55.50. Redistribution subject to SEG license or copyright; see Terms of Use at http://library.seg.org/

We can then define azimuth with two components:
α = (image azimuth, acquisition azimuth)

Shown in Figure 5, are depth slices of the stacked RTM images of the SEG logo near the model base for the 3x3 combinations of data. Note, the highest quality images occur where the image azimuth and acquisition azimuth are the same. This is because the sail line spacing is coarser than the shot spacing within each acquisition azimuth.

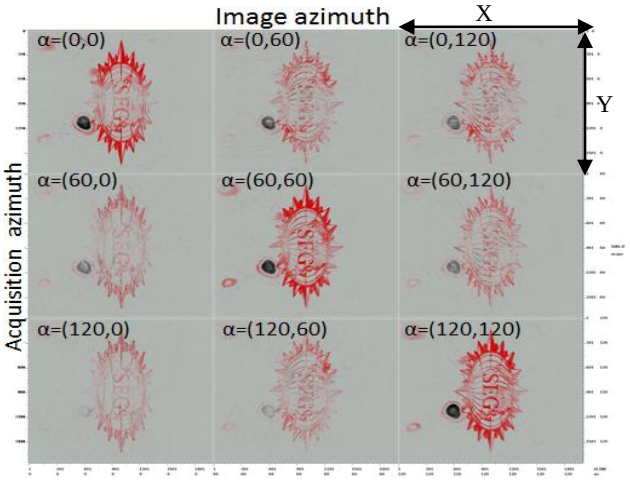

Figure 5: Depth slices from full azimuth RTM of SEAM synthetic. Each panel is a subset of the full azimuth data, where for each acquisition direction the data is binned into 3 image azimuths.

To further demonstrate the effects of image azimuth and acquisition azimuth, the 3x3 independent angle-azimuth stacks and angle gathers were created. Figure 6 below shows a line from a full angle-azimuth RTM stack. Note the red box around the subsalt area in this display. In this area we show more detailed displays of both angle gathers and angle stacks for all 3x3 combinations in Figure 7.

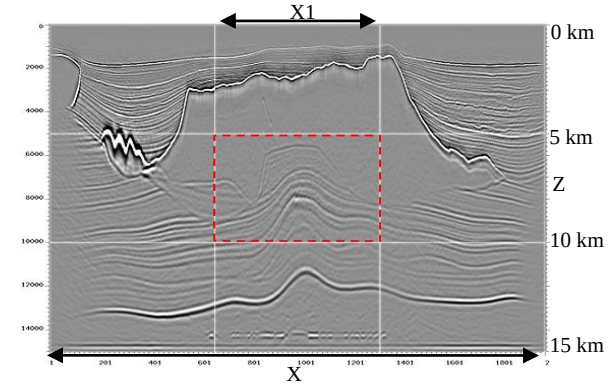

Figure 6: Stack of all RTM images for all of the input data. The red box is subsalt, where both angle gathers and angle stacks are examined for all combinations of image and acquisition azimuths as shown in Figure 7.

The displays in Figure 7 also show that the highest quality images occur when the image and the acquisition azimuths are the same. This affords the possibility of optimized processing methods based on the azimuth and angle decomposition of the data.

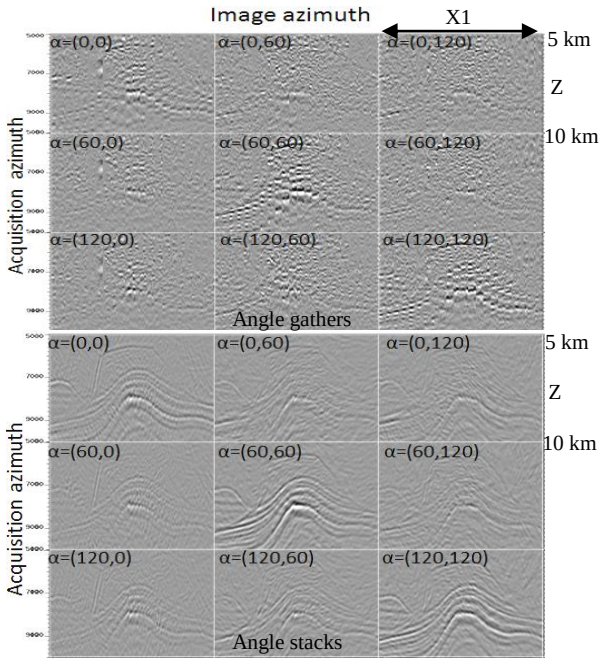

Figure 7: The frames above show the image and acquisition azimuths of the RTM images for the subsalt area highlighted in Figure 6. The top is a set of angle gathers (10 to 50 degrees) and the lower is a set of angle stacks (over all angles).

Conclusions

In this paper we have discussed the application of advanced imaging conditions and dynamic binning applied to reverse time migration. This inverse scattering condition reduces the RTM backscatter during propagation in the imaging process, which allows for improved angular binning.

We demonstrated the application of the angle-azimuth decomposition for use in processing, analysis and angle based tomography for wide and full azimuth data.

Acknowledgements

We thank PGS for permission to present this paper. We acknowledge the SEG for the use of the SEAM model and the PGS acquisition and processing groups for the planning, generation and imaging of the multi-azimuth synthetic. In particular we thank Morten Pedersen, Silke Bude, and Steve Campbell.

© 2014 SEG

DOI http://dx.doi.org/10.1190/segam2014-0876.1

http://dx.doi.org/10.1190/segam2014-0876.1

EDITED REFERENCES

Note: This reference list is a copy-edited version of the reference list submitted by the author. Reference lists for the 2014 SEG Technical Program Expanded Abstracts have been copy edited so that references provided with the online metadata for each paper will achieve a high degree of linking to cited sources that appear on the Web.

REFERENCES

Op 't Root, T., C. Stolk, and M. V. de Hoop, 2012, Linearized inverse scattering based on seismic reverse-time migration: Journal de Mathématiques Pures et Appliquées, **98**, no. 2, 211–238.

Tang, B., S. Xu, and Y. Zhang, 2011, Aliasing in RTM 3D angle gathers: 81st Annual International Meeting, SEG, Expanded Abstracts, 3310–3314.

Whitmore, N., and S. Crawley, 2012, Applications of RTM inverse scattering imaging conditions: 82nd Annual International Meeting, SEG, Expanded Abstracts, doi: 10.1190/segam2012-0779.1.

Xu, S., Y. Zhang, and B. Tang, 2011, 3D angle gathers from reverse time migration: Geophysics, **76**, no. 2, S77–S92, http://dx.doi.org/10.1190/1.3536527.

Downloaded 09/09/15 to 62.252.55.50. Redistribution subject to SEG license or copyright; see Terms of Use at http://library.seg.org/